**University of Pennsylvania**
**ScholarlyCommons**

Departmental Papers (CBE)

Department of Chemical & Biomolecular Engineering

1-1-2010

# Fabrication of LSM-YSZ Composite Electrodes by Electrodeposition

Fred Bidrawn
*University of Pennsylvania*, fbidrawn@seas.upenn.edu

John M. Vohs
*University of Pennsylvania*, vohs@seas.upenn.edu

Raymond J. Gorte
*University of Pennsylvania*, gorte@seas.upenn.edu

# Fabrication of LSM-YSZ Composite Electrodes by Electrodeposition

**Abstract**

Composites of Sr-doped $LaMnO_3$ (LSM) and yttria-stabilized zirconia (YSZ) were prepared by sequential electrodeposition of La and Mn species from nitrate salts in Dimethyl Sulfoxide (DMSO) into porous, carbon-coated YSZ substrate, followed by the infiltration of $Sr(NO_3)_2$. The La and Mn species were uniformly deposited throughout the depth of 50 μm porous layer to the interface with a dense YSZ electrolyte. The LSM perovskite phase was formed after heating to 1373 K. Solid oxide fuel cell cathodes prepared by single-step electrodeposition showed similar performance to LSM-YSZ electrodes prepared by wet impregnation using many steps.

**Disciplines**
Physical Sciences and Mathematics | Physics

# Fabrication of LSM–YSZ Composite Electrodes by Electrodeposition

**F. Bidrawn, J. M. Vohs,\* and R. J. Gorte\*,z**

*Department of Chemical and Biomolecular Engineering, University of Pennsylvania, Philadelphia, Pennsylvania 19104, USA*

Composites of Sr-doped LaMnO$_3$ (LSM) and yttria-stabilized zirconia (YSZ) were prepared by sequential electrodeposition of La and Mn species from nitrate salts in Dimethyl Sulfoxide (DMSO) into a porous, carbon-coated YSZ substrate, followed by the infiltration of Sr(NO$_3$)$_2$. The La and Mn species were uniformly deposited throughout the depth of a 50 μm porous layer to the interface with a dense YSZ electrolyte. The LSM perovskite phase was formed after heating to 1373 K. Solid oxide fuel cell cathodes prepared by single-step electrodeposition showed similar performance to LSM–YSZ electrodes prepared by wet impregnation using many steps.

© 2010 The Electrochemical Society. [DOI: 10.1149/1.3484096] All rights reserved.

Composites of Sr-doped LaMnO$_3$ (LSM) and yttria-stabilized zirconia (YSZ) are the most commonly used materials for cathodes in solid oxide fuel cells that are based on YSZ electrolytes, even though improved performance could be achieved by replacing LSM with mixed-conducting perovskites.[1-6] The primary reasons for using LSM are that LSM has a similar coefficient of thermal expansion as YSZ and that LSM and YSZ are relatively unreactive, so mixed powders can be fired to 1473 K without causing a significant level of solid-state reaction.[7] The ability to calcine the mixed powders to high temperatures is particularly important because it greatly simplifies the fabrication of LSM–YSZ electrodes. LSM–YSZ electrodes are often produced by screen printing a mixture of LSM and YSZ powders onto a dense YSZ electrolyte, followed by calcination. By calcining to relatively high temperatures, the YSZ within the electrode is sintered to the YSZ electrolyte, providing ion-conducting channels that increase the length of the three-phase boundary.[8]

Recently, an alternative method for the fabrication of composite electrodes has been developed in which the perovskite is added into a porous YSZ scaffold by infiltration after the scaffold has been sintered onto the YSZ electrolyte.[9-12] The primary advantage of this method is that high temperatures can be used to sinter the YSZ component of the electrode to the electrolyte, while using lower temperatures for the perovskite component so as to avoid solid-state reactions with the YSZ and maintain the perovskite phase in nano-crystalline form.[13] Because the structure of composites formed by infiltration is not random, it is also possible to use less of the perovskite phase to achieve conductivity.[8,14]

The primary disadvantage of fabrication by infiltration is that the process is tedious because multiple infiltration and calcination steps are required. The maximum amount of perovskite that can be added in a single step is equal to that which can be formed from the volume of liquid required to fill the pore volume of the YSZ scaffold. Therefore, it is easy to calculate that infiltration of 1 M solutions of La$^{+3}$ and Mn$^{+3}$ into a 65% porous scaffold produce only 2.3 vol % LaMnO$_3$.[8] A single-step infiltration of a 15 wt % solution of LaMnO$_3$ nanoparticles produces an even lower loading of the perovskite.[15,16] Even though less of the perovskite is required to achieve the percolation threshold in composites formed by infiltration,[14] apparently, loadings should at least approach the percolation threshold for normal composite electrodes, ∼30 vol %.

Higher loadings of the conductive phase can be achieved in a single step by electrodeposition. For example, metal–YSZ composites with relatively high loadings of Cu, Co, or Ni have been prepared by electrodeposition of the metals onto porous YSZ scaffolds that had been coated with a thin layer of carbon to make them

conductive.[17] While electrodeposition has not yet been used to synthesize perovskite-based electrodes, LaMnO$_3$ has been electroplated onto flat surfaces.[18-21] Therefore, the present study set out to demonstrate that LSM–YSZ composites could also be produced in this way.

Ensuring that deposition occurs uniformly throughout the porous electrode, not simply on the external surface, is challenging; the necessary conditions for accomplishing this have been outlined in previous papers.[17,22] Because most of the potential drop in electroplating occurs within a few nanometers of the solid surface,[23] the potential in the fluid at the center of the micrometer-sized pores that make up the porous electrode must be uniform and similar to that of the bulk solution into which the porous substrate is immersed. This requires that the conductivity of the solution be high and that the concentration of cations in the solution be uniform throughout the bulk fluid and at the center of the pores.[17] In the absence of significant field gradients, the migration of ions into the pores from the external solution is controlled primarily by molecular diffusion because convection is negligible in micrometer-sized channels. Therefore, it is necessary to control the concentration of the plating solution to maximize conductivity and to use low currents so that diffusion of ions into the pores is rapid compared to the rate of deposition.

We show that it is possible to use electrodeposition to achieve sufficiently high loadings of La and Mn so that a conductive electrode can be formed in a single electrodeposition step. Because we were unable to deposit La as a metallic species, the amount of La that we were able to deposit was limited by the formation of an insulating film.

## Experimental

The fuel cells used in this work were prepared from YSZ wafers that had a dense electrolyte layer separating two porous layers, as described in other publications.[24] The porous–dense–porous wafers were prepared by laminating three green tapes with the outside tapes containing graphite pore formers, followed by sintering of the tapes at 1773 K for 4 h. In the present study, the dense electrolyte layers were 100 μm thick and 1 cm in diameter, while the two porous layers were 50 μm thick each and 0.67 cm in diameter. Based on an earlier work, the porous layers were ∼65% porous.[25]

The cathodes of the fuel cells were synthesized by adding LSM (La$_{0.8}$Sr$_{0.2}$MnO$_3$) to one of the porous layers by either aqueous infiltration or electrodeposition. With aqueous infiltration, a solution with the correct stoichiometric mixture of La, Sr, and Mn nitrate salts was added to the porous YSZ scaffold and then heated to 723 K to remove the water and decompose the nitrates.[7] This cycle was repeated until the loading was 40 wt % of the added oxide. Finally, the added oxide was heated to 1373 K to form the perovskite phase.

When adding LSM by electrodeposition, it was first necessary to make the YSZ scaffold electronically conductive. This was accom-

\* Electrochemical Society Active Member.

z E-mail: gorte@seas.upenn.edu

plished by placing the sintered cell in flowing butane at 1123 K until ~2 wt % of conductive carbon had been deposited in the pores.[17] Assuming a density of 1 g/cm³ for the carbon, 2 wt % corresponds to 15 vol % of the scaffold or 23% of the available pore volume within the YSZ. The scaffold was not sufficiently conductive with less than 2 wt % carbon; depositing more than 2 wt % carbon resulted in significant filling of the YSZ pores, which limited the amount of material that could be added by electrodeposition. Following carbon deposition, a silver wire was attached with silver paste to the edge of the YSZ scaffold that would become the cathode. Candle wax was used to cover the silver wire and paste, as well as the opposing YSZ scaffold that would become the anode.

Before attempting to deposit La into the porous scaffold, experiments were performed on a flat stainless steel foil to understand the nature of the deposits. Although there are papers that claim metallic La can be electrodeposited, even from aqueous solutions,[26,27] we found the process to be more complex. Our initial attempts to deposit La used aqueous solutions of La(NO₃)₃ containing sodium citrate, sodium tartarate, or ethylenediaminetetraacetic acid; all of these produced a thin gel-like coating on the foil. The deposits were almost certainly La(OH)₃, as reported by Therese and Kamath,[19] produced indirectly through the reduction of oxygen in the electrolyte.[28] Similar results were obtained using glacial acetic acid as the solvent. Finally, deposition was attempted using anhydrous LaCl₃ in DMSO (Fisher Scientific),[29-31] dimethylformamide (Fisher Scientific),[32] and ethylenediamene (Alfa Aesar).[33] The experiments carried out with DMSO were conducted in a dry box under a N₂ atmosphere after passing the DMSO through a bed of 4 A molecular sieve. Although the use of dry organic solvents eliminated H₂ evolution at the electrode, the nature of the deposits was unchanged. For the present application, deposition of the hydroxide was considered acceptable.

Electrodeposition was accomplished using a two-electrode electrochemical cell with a Pt counter electrode. The Mn and La species were deposited separately using 0.1 M solutions of their respective nitrate salts in DMSO. For the composite La–Mn cell, deposition was performed consecutively, with the Mn deposited first because it deposited as a metal, immediately followed by La. In this study, all depositions were carried out galvanostatically at a current density of 4.5 mA/cm². All deposition quantities in this paper were determined from measured weight changes in the sample. Once deposition was complete, the silver leads were detached and SrO was added by a single infiltration of Sr(NO₃)₂. Finally, the cells were calcined to either 1123 or 1373 K, temperatures that were sufficient to remove the deposited carbon and the candle wax.

For fuel-cell testing, ceria and Pd were infiltrated into the porous YSZ on the anode side after LSM had been added to the cathode side to a final composition of 50 and 0.5 wt % CeO₂ and Pd, respectively, as described elsewhere.[25] The final calcination temperature for the anode was 973 K. Cells were then mounted onto an alumina tube and tested at 973 K with the anode in flowing, humidified (3% H₂O) H₂ and the cathode simply exposed to the laboratory air. Impedance spectra and voltage–current density (*V-i*) polarization curves were measured using a Gamry Instruments potentiostat. Impedance spectra were measured galvanostatically at various currents in the frequency range of 300 kHz–0.1 Hz with a 1 mA ac perturbation.

Following the preparation of various electrodes, characterization of the bulk phases was conducted using X-ray diffraction (XRD), while the morphology and uniformity of the deposits were examined by scanning electron microscopy (SEM) with energy-dispersive X-ray spectroscopy (EDX).

### Results and Discussion

To determine the conditions for achieving homogenous deposition of each species, Mn and La were each electrodeposited onto separate, carbon-coated YSZ substrates. Figure 1 shows deposition curves for Mn and La using 0.1 M nitrate solutions in DMSO. No
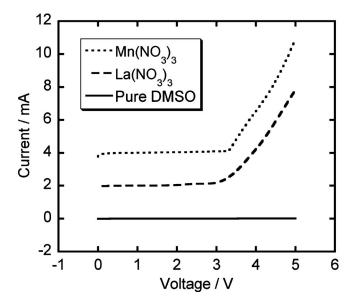


**Figure 1.** Deposition curves for pure DMSO and for 0.1 M solutions of Mn(NO₃)₃ and La(NO₃)₃ in DMSO. Data for Mn and La solutions have been offset for clarity.

current was observed for the pure DMSO for potentials below 10 V, while deposition on the fresh substrates occurred for both the Mn and La solutions beginning at ~3.5 V. However, for both Mn and La solutions, the deposition currents at a constant potential of 4.0 V decreased with time over the period of several hours well before the desired loadings of either component had been achieved, such that it was not practical to perform deposition in the potentiostatic mode. Therefore, deposition was performed galvanostatically with a current density of 4.5 mA/cm². As shown later, this current density was sufficiently low to allow uniform deposition throughout the porous scaffold and could be maintained to reasonable loadings for both Mn and La.

With Mn, the initial voltage was ~4 V and increased to ~5 V as the Mn deposited inside the electrode pores. Once the pore volume had been filled, the voltage increased rapidly to above 10 V and deposits began forming externally on the electrode surface. Internal Mn loadings of as high as ~60 wt % Mn₂O₃ were obtained. The average coulomb efficiency of deposition inside the electrode pores was ~30%.

The characteristics of La deposition were quite different. While the initial voltage required for 4.5 mA/cm² was also ~4 V, the voltage rose and reached a plateau after 10 min at a value near 5 V. The loading at this point was equivalent to ~20 wt % La₂O₃ with an average coulomb efficiency of 20%. Beyond this time, no further deposition occurred either in the pores or on the external surface, even though the current remained constant. Particles of La(OH)₃ possibly continued to form after this time but remained as colloidal particles in solution, external to the pore structure and separate from the sample.

We attempted to characterize the Mn and La by XRD immediately following the room-temperature deposition but the deposits were amorphous. The cells were then calcined in air to 1123 K to remove carbon and oxidize the deposits to either Mn₂O₃ or La₂O₃. The SEM micrographs of these oxidized deposits taken at a depth of 40 μm from the external surface of the scaffold and 10 μm from the dense electrolyte layer are shown in Fig. 2. For comparison purposes, Fig. 2a is an image of the porous YSZ scaffold and shows that the scaffold is made up of relatively uniform pores between 1 and 3 μm. With the addition of Mn, Fig. 2b, the YSZ scaffold is covered with a layer of Mn₂O₃ particles ~0.2 μm. The uniformity of the layer suggests that it was probably formed by the oxidation of a thin film of the metallic Mn. The oxidized La deposits, Fig. 2c,
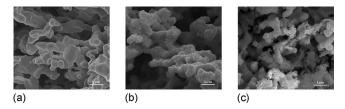
**Figure 2.** SEM images of a porous YSZ scaffold (a) before and after electrodeposition in solutions of (b) 0.1 M $Mn(NO_3)_3$ or (c) 0.1 M $La(NO_3)_3$ in DMSO. Deposited species were fired to 1123 K immediately following deposition.

exist as clumps within the scaffold structure. This is consistent with the picture that $La(OH)_3$ particles form in solution near the surface and simply precipitate inside the channels.

Because Mn apparently deposits in its metallic form as an even layer over the scaffold, the perovskites were prepared by electrodepositing Mn first, then adding the La. This allowed the conductivity of the scaffold to be maintained for the subsequent addition of La. The conditions used for sequential depositions were identical to that used for the deposition of the individual components. A loading of 30 wt % $LaMnO_3$ was targeted based in part on the results obtained for electrodeposition of the pure compounds, which suggested that this is the maximum realistic loading achievable for La and in part, on the fact that this loading is sufficient to provide the necessary conductivity for infiltrated-LSM electrodes.[14] The voltage–time characteristics were in qualitative agreement with the results obtained for the pure compounds. For a constant current density of 4.5 $mA/cm^2$, the voltage rose continuously over the duration of the Mn deposition; when the sample was placed in the La plating bath, the initial voltage was lower than the final voltage in the Mn bath but again rose to a plateau value at ~6.5 V in this case.

Figure 3 shows a SEM micrograph of the YSZ scaffold after deposition of both Mn and La to a loading of 33 wt %, following calcination to 1123 K. The deposits are in the form of small nanoparticles, spread uniformly over the YSZ scaffold. The EDX line scan, shown in Fig. 4, demonstrates that the La and Mn are present together down to the interface with the YSZ electrolyte.

To confirm that the deposited species had formed the desired perovskite phase following calcination, XRD data were taken from the electrode prepared by electrodeposition and compared to that of an LSM electrode prepared by infiltration to a loading of 40 wt %
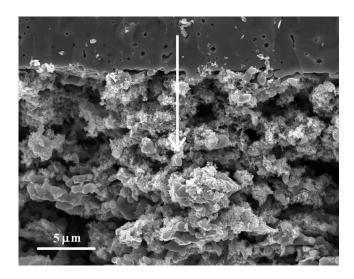


**Figure 3.** SEM micrograph showing the porous YSZ scaffold following sequential electrodeposition in solutions of 0.1 M $Mn(NO_3)_3$ and 0.1 M $La(NO_3)_3$ in DMSO, then calcined to 1123 K.
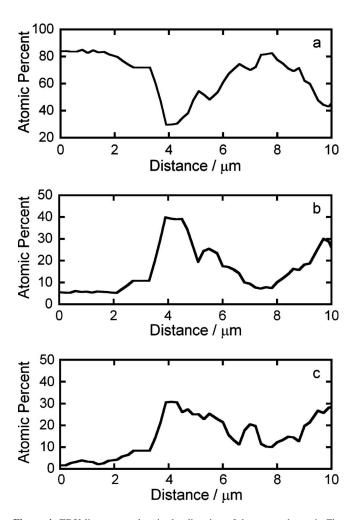


**Figure 4.** EDX line scans taken in the direction of the arrow shown in Fig. 3. Species measured are (a) Zr, (b) La, and (c) Mn.

LSM. Both diffraction patterns were taken after calcination to 1373 K and are presented in Fig. 5. Both patterns show a broad peak at ~32.5 2θ corresponding to the perovskite phase. The relative intensity of the perovskite peak to that of the YSZ peak was smaller for the composite prepared by electrodeposition, partly because the loading was lower. However, because salts added by infiltration tend to be pulled to the external surface of the scaffold during the drying process,[34] the smaller intensity of the diffraction line following electrodeposition is due to the perovskite forming more deeply into the scaffold, closer to the electrolyte.

To determine how well composites formed by electrodeposition could perform as fuel-cell electrodes, otherwise identical fuel cells were prepared using electrodeposition and normal infiltration by nitrate salts. For these experiments, an aqueous solution of $Sr(NO_3)_2$ was introduced into the scaffold containing the electrodeposited La and Mn before calcination to produce a composition as close as possible to $La_{0.8}Sr_{0.2}MnO_3$, although it is difficult to achieve the targeted composition precisely using electrodeposition. For both preparation methods, LSM–YSZ composites were calcined to 1373 K before adding 50 and 0.5 wt % ceria and Pd, respectively, in the anode. The cells were then tested in humidified (3% $H_2O$) $H_2$ at 973 K while holding the cathode in air.

Figures 6 and 7 provide a comparison of V-*i* polarization curves and impedance plots for cells prepared by electrodeposition and normal infiltration. The results demonstrate that the performance of both LSM electrodes is essentially identical. Because the performance of LSM–YSZ electrodes changes after polarization,[7] data are shown starting from open circuit and after shorting the cells for 2 h.
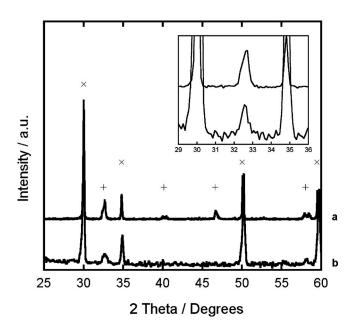
**Figure 5.** XRD data for LSM–YSZ composites prepared by (a) wet impregnation and (b) electrodeposition. Peaks marked by ($\times$) correspond to YSZ. Peaks marked by + correspond to undoped $LaMnO_3$.



**Figure 7.** *V-i* polarization plots measured at 973 K for cells with cathodes prepared by ($\blacklozenge$) wet impregnation and ($\bullet$) electrodeposition. Data are shown for both cells before (open symbols) and after (closed symbols) polarization by shorting the cells for 2 h.

Starting from open circuit, the V-*i* relationships in Fig. 7 are highly curved, with slopes decreasing with current density. After shorting for 2 h, the V-*i* dependences are nearly linear. The impedance curves in Fig. 6, measured at open circuit before and after shorting, show that the ohmic losses are 0.45 $\Omega$ cm$^2$ for the impregnated cell and unaffected by shorting. This value agrees well with the resistance expected for the 100 $\mu$m YSZ electrolytes. The ohmic losses of the electrodeposited cell were slightly higher at 0.65 $\Omega$ cm$^2$ and decreased to 0.55 $\Omega$ cm$^2$ after shorting. This increased ohmic loss is likely due to insufficient weight loading of the perovskite within the

electrode. The most prominent effect of shorting was on the nonohmic impedances, which decreased from 2.1 to ~0.6 $\Omega$ cm$^2$, with most of this coming from the LSM cathodes.[35]

To demonstrate that it was not simply the silver paste that was acting as the cathode, we also tested a cell that was identical to the ones for which data are shown in Fig. 6 and 7, except that no LSM was added on the cathode side. At 973 K, this cell exhibited an ohmic loss of 2.5 $\Omega$ cm$^2$ and an impedance that was independent of current density. Assuming 2 $\Omega$ cm$^2$ of the ohmic losses come from the empty YSZ scaffold, the conductivity of the 50 $\mu$m porous YSZ is calculated to be 0.0025 S/cm. This is 10 times lower than that of the nonporous YSZ at 973 K.[24] The result also demonstrates that the LSM added by electrodeposition provides conductivity to the electrode. Previous papers have discussed possible reasons for LSM activation by polarization and these are not repeated here.[7,36,37] Of primary importance for the present study is that the LSM added by electrodeposition shows identical performance to normally infiltrated LSM.

While we chose to prepare LSM–YSZ electrodes in this present study, electrodeposition could have been used to prepare electrodes with other compositions as well.

## Conclusion

Previous work has shown that infiltration of perovskites or perovskite precursors into a YSZ scaffold can produce electrode materials with improved properties over traditional composites formed by sintering of mixed powders; however, the infiltration procedure must typically be repeated many times to achieve the necessary loading of the perovskite. It is possible to prepare similar perovskite–YSZ composites by electrodeposition. The weight loading achieved in this study was limited by the fact that La deposited as a hydroxide and could be improved by electrodeposition of the metallic La.
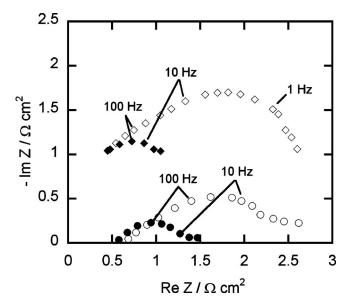
## Acknowledgment

**Figure 6.** Impedance data measured at open circuit for cells with cathodes prepared by ($\blacklozenge$) wet impregnation and ($\bullet$) electrodeposition. Data are shown for both cells before (open symbols) and after (closed symbols) polarization by shorting the cells for 2 h. The data were obtained at 973 K, and the spectra for the cell prepared by wet impregnation have been offset for clarity.
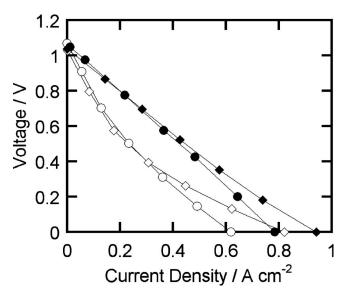
## References

1. T. Horita, K. Yamaji, N. Sakai, H. Yokokawa, A. Weber, and E. Ivers-Tiffee, *Electrochim. Acta*, **46**, 1837 (2001).
2. S. P. Simner, J. F. Bonnett, N. L. Canfield, K. D. Meinhardt, V. L. Sprenkle, and J. W. Stevenson, *Electrochem. Solid-State Lett.*, **5**, A173 (2002).
3. S. P. Simner, J. F. Bonnett, N. L. Canfield, K. D. Meinhardt, J. P. Shelton, V. L. Sprenkle, and J. W. Stevenson, *J. Power Sources*, **113**, 1 (2003).
4. Y. Huang, J. M. Vohs, and R. J. Gorte, *J. Electrochem. Soc.*, **151**, A646 (2004).
5. S. P. Jiang, *Solid State Ionics*, **146**, 1 (2002).
6. W. Wang, Y. Huang, S. Jung, J. M. Vohs, and R. J. Gorte, *J. Electrochem. Soc.*, **153**, A2066 (2006).
7. Y. Huang, J. M. Vohs, and R. J. Gorte, *J. Electrochem. Soc.*, **152**, A1347 (2005).
8. J. M. Vohs and R. J. Gorte, *Adv. Mater.*, **21**, 943 (2009).
9. R. Craciun, R. J. Gorte, J. M. Vohs, C. Wang, and W. L. Worrell, *J. Electrochem. Soc.*, **146**, 4019 (1999).
10. H. Kim, C. Lu, W. L. Worrell, J. M. Vohs, and R. J. Gorte, *J. Electrochem. Soc.*, **149**, A247 (2002).
11. R. J. Gorte, S. Park, J. M. Vohs, and C. Wang, *Adv. Mater.*, **12**, 1465 (2000).
12. J. D. Nicholas and S. A. Barnett, *J. Electrochem. Soc.*, **157**, B536 (2010).
13. R. Küngas, F. Bidrawn, J. M. Vohs, and R. J. Gorte, *Electrochem. Solid-State Lett.*, **13**, B87 (2010).
14. H. P. He, Y. Huang, J. Regal, M. Boaro, J. M. Vohs, and R. J. Gorte, *J. Am. Ceram. Soc.*, **87**, 331 (2004).
15. T. Z. Sholklapper, C. Lu, C. P. Jacobson, S. J. Visco, and L. C. De Jonghe, *Electrochem. Solid-State Lett.*, **9**, A376 (2006).
16. T. Z. Sholklapper, V. Radmilovic, C. P. Jacobson, S. J. Visco, and L. C. De Jonghe, *Electrochem. Solid-State Lett.*, **10**, B74 (2007).
17. S. Jung, J. M. Vohs, and R. J. Gorte, *J. Electrochem. Soc.*, **154**, B1270 (2007).
18. T. Sasaki, Y. Matsumoto, J. Hombo, and Y. Ogawa, *J. Solid State Chem.*, **91**, 61 (1991).
19. G. H. Therese and P. V. Kamath, *Chem. Mater.*, **10**, 3364 (1998).
20. G. H. Therese, M. Dinamani, and P. V. Kamath, *J. Appl. Electrochem.*, **35**, 459 (2005).
21. T. Mercer, P. A. J. de Groot, and P. N. Bartlett, *J. Appl. Electrochem.*, **28**, 455 (1998).
22. M. D. Gross, J. M. Vohs, and R. J. Gorte, *Electrochim. Acta*, **52**, 1951 (2007).
23. M. Paunovic and M. Schlesinger, *Fundamentals of Electrochemical Deposition*, p. 48, John Wiley & Sons, New York (2006).
24. F. Bidrawn, S. Lee, J. M. Vohs, and R. J. Gorte, *J. Electrochem. Soc.*, **155**, B660 (2008).
25. F. Bidrawn, G. Kim, N. Aramrueang, J. M. Vohs, and R. J. Gorte, *J. Power Sources*, **195**, 720 (2010).
26. A. S. Fouda and A. A. Al-Suhybani, *Orient. J. Chem.*, **1**, 5 (1985).
27. C. D. Lokhande, M. S. Jadhav, and S. H. Pawar, *Met. Finish.*, **86**, 53 (1988).
28. A. Q. Wang and T. D. Golden, *J. Electrochem. Soc.*, **150**, C616 (2003).
29. J. Butler, *J. Electroanal. Chem. Interfacial Electrochem.*, **14**, 89 (1967).
30. Y. Dingsheng, L. Guankun, and T. Yexiang, *J. Rare Earths*, **20**, 182 (2002).
31. D. Yuan and Y. Liu, *Mater. Chem. Phys.*, **96**, 79 (2006).
32. L. Martinot, L. Lopes, J. Marien, and C. Jerome, *J. Radioanal. Nucl. Chem.*, **253**, 407 (2002).
33. T. Moeller and P. A. Zimmerman, *Science*, **120**, 539 (1954).
34. S. Jung, C. Lu, H. He, K. Ahn, R. J. Gorte, and J. M. Vohs, *J. Power Sources*, **154**, 42 (2006).
35. M. D. Gross, J. M. Vohs, and R. J. Gorte, *Electrochem. Solid-State Lett.*, **10**, B65 (2007).
36. A. Hammouche, E. Siebert, A. Hammou, M. Kleitz, and A. Caneiro, *J. Electrochem. Soc.*, **138**, 1212 (1991).
37. E. Siebert, A. Hammouche, and M. Kleitz, *Electrochim. Acta*, **40**, 1741 (1995).